Accepted Manuscript

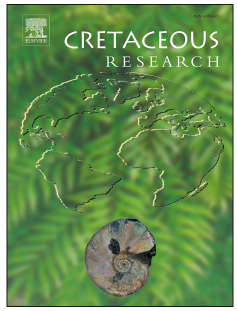

Correlation of Early Cretaceous radiolarian assemblages from southern Tibet and central Italy

Xin Li, Atsushi Matsuoka, Angela Bertinelli, Marco Chiari, Chengshan Wang

PII: S0195-6671(18)30324-0

DOI: https://doi.org/10.1016/j.cretres.2018.12.016

Reference: YCRES 4046

To appear in: *Cretaceous Research*

Received Date: 7 August 2018

Revised Date: 29 November 2018

Accepted Date: 30 December 2018

Please cite this article as: Li, X., Matsuoka, A., Bertinelli, A., Chiari, M., Wang, C., Correlation of Early Cretaceous radiolarian assemblages from southern Tibet and central Italy, *Cretaceous Research*, https://doi.org/10.1016/j.cretres.2018.12.016.

Correlation of Early Cretaceous radiolarian assemblages from southern Tibet and central Italy

Li Xin[a], Matsuoka Atsushi[b], Bertinelli Angela[c], Chiari Marco[d], and Wang Chengshan[e]

[a] State Key Laboratory of Palaeobiology and Stratigraphy, Nanjing Institute of Geology and Palaeontology and Center for Excellence in Life and Paleoenvironment, Chinese Academy of Sciences, Nanjing, 210008, China. xinli@nigpas.ac.cn

[b] Faculty of Science, Niigata University, Niigata, 950-2181, Japan

[c] Dipartimento di Fisica e Geologia, Università degli Studi di Perugia, Via A. Pascoli snc, Perugia, 06123, Italy

[d] C.N.R., Istituto di Geoscienze e Georisorse, sede secondaria, via G. La Pira 4, Firenze, 50121, Italy

[e] Department of Earth Science and Resources, China University of Geosciences, Beijing, 100083, China

Corresponding author: Li Xin

xinli@nigpas.ac.cn

Nanjing Institute of Geology and Palaeontology and Center for Excellence in Life and Paleoenvironment, Chinese Academy of Sciences, 39 East Beijing Road, Nanjing 210008, China.

ABSTRACT

Comparison of radiolarian assemblages from marls in the Gorgo a Cerbara section in the Umbria–Marche Basin in central Italy and a siliceous sequence (BB1 section) near Babazhadong in southern Tibet indicates similar faunas comparable to those in the *Aurisaturnalis carinatus* zone and *Turbocapsula costata* zone. Several significant species, *Archaeodictyomitra lacrimula* (Foreman), *A. excellens* (Tan Sin Hok), *Dictyomitra communis* (Squinabol), and *Aurisaturnalis carinatus perforatus* Dumitrica and Dumitrica-Jud, which are common in older strata, make their last occurrences near the base of the *Turbocapsula costata* zone in these two areas. Comparison with the Gorgo a Cerbara section provides an accurate age constraint for the siliceous succession in southern Tibet, which contains no fossils other than radiolarians. The comparison indicates a close connection between the western and eastern Tethys during the Barremian to early Aptian. The correlation testifies that the radiolarian zonation in southern Tibet is applicable for the whole Tethys. The siliceous succession in BB1 section encompasses the early Aptian Oceanic Anoxic Event 1a (OAE 1a). The early Aptian OAE 1a is located in the upper part of the *Aurisaturnalis carinatus perforatus* subzone. The first occurrence biohorizon of the genus *Turbocapsula* and the evolutionary first appearance biohorizon of *T. costata costata* (Wu) are useful markers for constraining the OAE 1a in the Tethys.

Keyword: early Aptian, Umbria–Marche Basin, southern Tibet, radiolarian assemblages, Oceanic Anoxic Event 1a

1. Introduction

O'Dogherty (1994) proposed a valuable mid-Cretaceous radiolarian zonation for the western Tethys based on radiolarian biostratigraphic study on the Northern Apennines and Betic Cordillera. Matsuoka et al. (2002) correlated their youngest radiolarian assemblage from the Xialu Chert in southern Tibet with the *Costata* subzone of O'Dogherty (1994) and named it "*Turbocapsula costata* zone". Wu (2007) pointed out that the specimens of *T. costata* described by Wu (1986) and O'Dogherty (1994) are in fact likely to be two different species and assignable to different ages. Li et al. (2017) remarked that Wu's and O'Dogherty's specimens are assigned to two different subspecies within a single species. The *Aurisaturnalis carinatus* zone and the *Turbocapsula costata* zone are defined based on radiolarian biostratigraphic study on siliceous sequence in southern Tibet. The *Turbocapsula costata* zone is subdivided into the *Turbocapsula costata multicostata* subzone and the *Turbocapsula costata costata* subzone by the evolutionary first appearance bio-horizion (EFAB) of *T. costata costata*. So far there are still controversy on age assignment for *Turbocapsula costata* (Wu). Although Lower Cretaceous radiolarian bearing strata are widely distributed in southern Tibet, they contain no fossils other than radiolarians. The radiolarian assemblages from the Apennines and Betic Cordillera, on the other hand, are well dated with nannofossil (Bralower et al., 1989; Coccioni et al., 1992, 2012; Erba, 1994) and planktic foraminifera (Coccioni et al., 1992, 2006；Patruno et al., 2015). No detailed correlation of radiolarian assemblages between the western and eastern Tethys was conducted to testify the applicability of the radiolarian zonation in southern Tibet for the whole Tethys.

The early Aptian Oceanic Anoxic Event (OAE) is characterized by considerable environmental and climate changes (Erba, 1994; Leckie et al., 2002; Erba et al., 2015). Black mudstone with high organic matter content, which is lithological expression of the OAE 1a in the western Tethys, is absent in coeval pelagic sequences in the Shimanto Belt in Japan (Ihoriya et al., 2009) and siliceous sequence in southern Tibet. Radiolarian biostratigraphy is a key method to indicate the early Aptian OAE 1a horizon in the siliceous sequence in southern Tibet.

The stratigraphic record of the Babazhadong 1 (BB1) section in southern Tibet and the Gorgo a Cerbara section in central Italy offers a good opportunity to correlate the radiolarian biostratigraphy between the eastern and western Tethys.

The main purposes of this study are: (1) To compare Early Cretaceous radiolarian assemblages from central Italy and southern Tibet, (2) To testify the applicability of the radiolarian zonation in southern Tibet for the whole Tethys, (3) To select radiolarian events useful for constraining the early Aptian Oceanic Anoxic Event 1a (OAE 1a).

2. Geological setting

The Tethyan Himalaya, which is located between the Higher Himalaya to the south and the Indus–Yarlung Tsangpo Suture to the north, was a part of the northern margin of the Greater India continental plate during the Cretaceous (Gansser, 1964; Wang et al., 1996) (Location 1 in Figs. 1, 2). It is roughly separated into two tectonic subzones by a line along the Gyirong–Kangmar Intracrustal Thrust. The southern subzone is characterized by shallow-water carbonate and clastic sediments (Wan et al., 2000), while the northern subzone is characterized by pelagic siltstones, cherts, and mudstones (Liu and Einsele, 1994; Hu et al., 2008). The Upper Jurassic to Upper Cretaceous strata of the northern subzone are divided into four formations: Upper Jurassic quartz sandstones of the Weimei Formation, Lower Cretaceous volcaniclastic litharenite intercalated with mudstones of the Rilang Formation, Lower–Upper Cretaceous siliceous mudstones and cherts of the Duobeng Formation, and Upper Cretaceous red beds of the Chuangde Formation (Du et al., 2015). The Babazhadong 1 (BB1) section, which is located near Babazhadong County, belongs to the northern subzone of the Tethyan Himalaya. This section is represented by the siliceous mudstones and cherts of the Duobeng Formation and was studied for radiolarians by Li et al. (2017).

The Umbria–Marche Basin is a Triassic to Messinian extensional basin, developed on the southern margin of the western Tethys and then of the Alpine–Apennine foreland, on the northern edge of the African Apulian plate, which belongs to the so called Adriatic Promontory (Channell et al., 1979; Muttoni et al., 2001; Patruno et al., 2015) (Location 2 in Figs. 1, 2). Jurassic to Paleocene pelagic to hemipelagic sediments were deposited at bathyal depths in the Umbria–Marche Basin. The Maiolica Formation (Tithonian to lower Aptian) consists dominantly of whitish pelagic limestone beds including black chert layers and nodules. The upper Aptian and Albian are represented mainly by polychrome marls of the Marne a Fucoidi

Formation. Gorgo a Cerbara is a well-studied section in the Umbria–Marche Basin (Fig. 3). The section encompasses the transition between the Maiolica and Marne a Fucoidi formations. The Selli Level in the upper part of the section is dominated by black and organic-rich claystones, variegated claystones, and radiolarites. Studies on the magnetostratigraphy (Lowrie et al., 1980; Speranza et al., 2005; Satolli et al., 2007, 2008), chemostratigraphy (Patruno et al., 2015; Erba, 1994), and cyclostratigraphy (Stein et al., 2011) of the section have been conducted. Detailed nannofossil (Bralower et al., 1989; Coccioni et al., 1992, 2012; Erba, 1994) and planktic foraminiferal (Coccioni et al., 1992, 2006；Patruno et al., 2015) biostratigraphic schemes have been established, additionally associated with ammonite (Cecca et al., 1994; Channell et al., 1995), calpionellid (Monechi, 1989), and radiolarian data (Erbacher, 1994; O'Dogherty, 1994).

3. Material and Methods

The Babazhadong 1 section is located 6 km northwest of the Babazhadong County. In this study, we follow the logged columnar section and radiolarian biostratigrahy of Li et al. (2017). The strata trend NW–SE and dip to the north.

The Gorgo a Cerbara section (43°36′01″N, 12°33′16″E) is located along the right bank of the Candigliano River, 4 km east of the town of Piobbico, central Italy. In this work, we follow the logged columnar section and dataset of Patruno et al. (2011; 2015). A total of 20 samples were gathered from this section (Fig. 3).

For the limestones of the Maiolica Formation, rock samples were treated with 8%

hydrochloric acid (HCl) for 1 h. For marls of the Marne a Fucoidi and cherts from the southern Tibet, we used the standard hydrofluoric acid (HF) method (Pessagno and Newport, 1972). Rock samples were disaggregated by 5% HF for 20–24 h. The 63–380-μm fractions were used to obtain radiolarian-containing residues. Two samples from the Gorgo a Cerbara section and 16 samples from the Babazhadong 1 section yielding moderately to well-preserved radiolarians were studied to determine the stratigraphic range of radiolarian species. Radiolarian specimens were picked up under a stereoscopic microscope and a transmitted light microscope was used to observe the inner structures of the radiolarians. A total of 1800 Scanning electron microscope images and 2000 light microscope images were used for the biostratigraphic analysis of the radiolarians. Radiolarian assemblages from the two corresponding horizons of the Gorgo a Cerbara section and the Babazhadong 1 section are examined for comparison.

4. Early Cretaceous radiolarian occurrence and biostratigraphy

The Babazhadong 1 (BB1) section in southern Tibet yields abundant radiolarians. The preservation varies among samples. The faunal composition is similar to that in the Gorgo a Cerbara section, central Italy (Table 1).

4.1. Babazhadong 1 section

A total of 25 samples were collected from the BB1 section. Twelve samples yielding moderately to well-preserved radiolarians were studied for radiolarian biostratigraphy and the phyletic evolution of the genus *Turbocapsula*. Based on the phyletic evolution of *Aurisaturnalis* and *Turbocapsula*, two radiolarian zones have been defined: the *Aurisaturnalis carinatus* zone and the *Turbocapsula costata* zone (Li et al., 2017). In this study, two radiolarian assemblages: one comparable to the *Aurisaturnalis carinatus* zone (BB1-011, Fig. 4) and the other one comparable to the *Turbocapsula costata* zone (BB1-021, Fig. 5) are analyzed for comparison.

Radiolarian fauna from sample BB1-11 is characterized by the occurrence of *Archaeodictyomitra lacrimula* (Foreman), *Archaeodictyomitra excellens* (Tan Sin Hok), *Dictyomitra communis* (Squinabol), *Pseudocrolanium puga* (Schaaf), *Acaeniotyle umbilicata* (Rüst), *Aurisaturnalis carinatus perforatus* Dumitrica and Dumitrica–Jud, *Dicerosaturnalis amissus* (Squinabol), *Pseudodictyomitra recta* Vishnevskaya, *Stichomitra communis* Squinabol, *Neorelumbra manokawaensis* (Tumanda), *Thanarla pacifica* Nakaseko and Nishimura, *Xitus alievi* (Foreman), *Squinabollum asseni* (Tan Sin Hok), *Hiscocapsa grutterinki* (Tan Sin Hok), *Arcanicapsa clivosa* (Aliev), *Turbocapsula tetras* Li and Matsuoka, *Pseudoeucyrtis hanni* (Tan Sin Hok), *Mictyoditra columbarium* (Renz), *Suna echiodes* (Foreman), *Archaeospongoprunum patricki* Jud, *Acastea diaphorogona* (Foreman), *Quinquecapsularia* sp., *Conocaryomma* sp. B in Thurow (1988), *Becus horridus* (Squinabol), *Emiluvia* sp., *Dactyliosphaera* sp., and *Halesium* sp.

Radiolarian fauna from sample BB1-021 is characterized by the occurrence of *Thanarla brouweri* (Tan Sin Hok), *Pseudocrolanium puga* (Schaaf), *Pseudodictyomitra recta* Vishnevskaya, *Pseudodictyomitra hornatissima* (Squinabol), *Xitus clava* (Parona), *Stichomitra communis* Squinabol, *Turbocapsula costata costata* (Wu), *Turbocapsula fugitiva* O'Dogherty, *Hiscocapsa grutterinki* (Tan Sin Hok), *Squinabollum asseni* (Tan Sin Hok), *Pseudoeucyrtis hanni* (Tan Sin Hok), *Mictyoditra columbarium* (Renz), *Mesosaturnalis* sp., *Dicerosaturnalis amissus* (Squinabol), *Acastea diaphorogona* (Foreman), *Suna hybum* (Foreman), *Becus horridus* (Squinabol), *Pantanellium squinaboli* (Tan Sin Hok), *Archaeospongoprunum patricki* Jud, *Acaeniotyle umbilicata* (Rüst), *Halesium* sp., *Conocaryomma* sp. B in Thurow (1988), *Holocryptocanium tuberculatum* Dumitrica, and *Deviatus diamphidius* (Foreman), *Acastea* sp., *Suna* sp., and *Conocaryomma* sp.

4.2. Gorgo a Cerbara section

A total of 20 samples were collected from the Gorgo a Cerbara section. Only 2 samples yielding moderately to well-preserved radiolarians were used for radiolarian biostratigraphic comparison in this study. Two distinct radiolarian assemblages are recognized from these two samples: the *Aurisaturnalis carinatus* zone (GC-025, Fig. 6) and the *Turbocapsula costata* zone (GC-007, Fig. 7).

Sample GC-025 yielded *Archaeodictyomitra lacrimula* (Foreman), *Archaeodictyomitra excellens* (Tan Sin Hok), *Dictyomitra communis* (Squinabol), *Crococapsa uterculus* (Parona), *Olanda orca* (Foreman), *Pantanellium squinaboli* (Tan Sin Hok), *Acaeniotyle umbilicata* (Rüst), *Aurisaturnalis carinatus perforatus* Dumitrica and Dumitrica–Jud, *Dicerosaturnalis amissus* (Squinabol), *Thanarla pacifica* Nakaseko and Nishimura, *Pseudodictyomitra nodocostata* Dumitrica, *Pseudodictyomitra nakasekoi* Taketani, *Xitus clava* (Parona), *Stichomitra communis*

Squinabol, *Neorelumbra manokawaensis* (Tumanda), *Squinabollum asseni* (Tan Sin Hok), *Hiscocapsa grutterinki* (Tan Sin Hok), *Arcanicapsa clivosa* (Aliev), *Pseudoeucyrtis hanni* (Tan Sin Hok), *Mictyoditra columbarium* (Renz), *Acastea diaphorogona* (Foreman), *Suna hybum* (Foreman), *Quinquecapsularia* sp., *Becus horridus* (Squinabol), *Dicroa macroxiphus* (Rüst), *Conocaryomma* sp. B in Thurow (1988), *Hiscocapsa*? sp., *Dactyliodiscus* sp., *Staurospaeretta* sp., and *Halesium* sp.

Sample GC-007 yielded *Thanarla brouweri* (Tan Sin Hok), *Dictyomitra communis* (Squinabol), *Pseudocrolanium puga* (Schaaf), *Pseudodictyomitra hornatissima* (Squinabol), *Xitus clava* (Parona), *Turbocapsula costata costata* (Wu), *Hiscocapsa grutterinki* (Tan Sin Hok), *Squinabollum asseni* (Tan Sin Hok), *Pseudoeucyrtis hanni* (Tan Sin Hok). *Mictyoditra columbarium* (Renz), *Hiscocapsa* sp., *Mesosaturnalis* sp., *Suna* sp., *Acastea* sp., *Conocaryomma* sp. B in Thurow (1988), *Holocryptocanium tuberculatum* Dumitrica, and *Dactyliodiscus florealis* (Jud).

5. Discussion

5.1. Comparison with previous radiolarian biostratigraphy in central Italy

Radiolarian zonation of the uppermost Barremian to lower Aptian (*Squinabollum asseni* zone and the *Turbocapsula* zone) was defined by O'Dogherty (1994) based mainly on his research in the Gorgo a Cerbara section. Stratigraphic occurrences of significant radiolarian taxa reported by O'Dogherty (1994) and this study are illustrated in Fig. 3. Stratigraphic occurrences of most species in this study are in accordance with those in O'Dogherty (1994) (Fig. 3 and Table 1).

The genus *Turbocapsula* is an index taxon of Barremian–Aptian radiolarians both for the western Tethys and the eastern Tethys, although there are still debates on its taxonomy and age assignment.

O'Dogherty (1994) pointed out that *T. costata* is a significant species of the Aptian radiolarian in the western Tethys. He proposed possible phyletic relationships of species belonging to the genus *Turbocapsula*: *T. giennensis* appears to have evolved from *T. fugitiva* and given rise to *T. costata*.

Turbocapsula costata is repeatedly reported from the ophiolite belt (Wu, 1986; Ziabrev et al., 2003), siliceous accretionary complex (Matsuoka et al., 2002; Ziabrev et al., 2004), and the passive margin sediments (Li et al., 2017) along the Yarlung–Tsangpo Suture Zone (YTSZ), southern Tibet. These deep marine sediments contain no fossils other than radiolarians. *Turbocapsula costata* is a key species for age assignment.

Specimens of *T. costata* described by Wu (1986) come from the Cenomanian Chongdui Formation in shouthern Tibet. Although the test outline of "*T. costata*" from the western Tethys and *Tricapsula costata* of the Chongdui Formation is similar, they are not one same species (Wu, 2007). Phyletic analyses of *T. costata* indicate that the specimens of Wu (1986) are assignable to *T. costata costata* and the specimens of O'Dogherty (1994) are assignable to *T. costata multicostata*. These two subspecies have different vertical distributions in BB1 section, but they co-occur in samples BB1-20 and BB1-021 (Li et al., 2017).

This study shows the existence of *Turbocapsula costata costata* (Wu) in Italy, which is comparable to typical specimens in the Chongdui Formation in southern Tibet. Only *Turbocapsula costata costata* occurs in GC-007, which is a little higher than BB1-021 and comparable to BB1-22 and BB1-025 in southern Tibet. This study testifies that the morphotypes of genus *Turbocapsula* and their biostratigraphic occurrences in southern Tibet are comparable to those in Italy. Therefore, the zonation established based on the phyletic evolution of the genus *Turbocapsula* is applicable for the western Tethys.

All figures of *T. costata* (pl.37, figs. 24–30) in O'Dogherty (1994) are from the Monte Casalini section. Because he did not distinguish the subspecies, it is difficult to know which subspecies he found in the Gorgo a Cerbara section. According to this study, only *T. costata costata* occurs in GC-007. Horizons of GC-911.35 and GC-914.00 in O'Dogherty (1994), which are higher than GC-007, specimens from these two samples are possibly *T. costata costata*. Compared with the results of O'Dogherty (1994), the evolutionary first appearance bio-horizion (EFAB) of *T. costata costata* in this study is 7 m lower and FOB of *S. communis* is 5 m lower.

5.2. Comparison of central Italy and southern Tibet

The base of the *Aurisaturnalis carinatus* zone is defined by the EFAB of *Aurisaturnalis carinatus carinatus* (Foreman) (Matsuoka, 1995; Dumitrica et al., 1997). This zone is divided into the *Aurisaturnalis carinatus carinatus* subzone and the *Aurisaturnalis carinatus perforatus* subzone on the basis of morphological change in *A. carinatus* (Dumitrica et al., 1997). The occurrence of *Aurisaturnalis carinatus perforatus* Dumitrica and Dumitrica-Jud in BB1-11 and GC-025 characterizes the *Aurisaturnalis carinatus perforatus* subzone.

A total of 20 species have been identified in green siliceous mudstone of BB1-11. The faunal contents are similar to those found in GC-025, which consists of whitish limestone beds including black chert nodules. BB1-11 records the first occurrence of *Turbocapsula tetras* Li and Matsuoka, which indicates the first occurrence of the genus *Turbocapsula*. GC-025 does not records the occurrence of the genus *Turbocapsula*, even we tried to find out it. GC-025 is possibly lower than BB1-11. Radiolarian assemblages, which are assignable to the *Aurisaturnalis carinatus perforatus* subzone, from the Umbria–Marche Basin and southern Tibet are characterized by the occurrence of *Archaeodictyomitra lacrimula* (Foreman), *Archaeodictyomitra excellens* (Tan Sin Hok), *Aurisaturnalis carinatus perforatus* Dumitrica, *Acaeniotyle umbilicata* (Rüst), *Dicerosaturnalis amissus* (Squinabol), *Stichomitra communis* Squinabol, *Neorelumbra manokawaensis* (Tumanda), *Thanarla pacifica* Nakaseko and Nishimura, *Squinabollum asseni* (Tan Sin Hok), *Hiscocapsa grutterinki* (Tan Sin Hok), *Arcanicapsa clivosa* (Aliev), *Pseudoeucyrtis hanni* (Tan Sin Hok), *Mictyoditra columbarium* (Renz), *Suna* sp., *Quinquecapsularia* sp., *Becus horridus* (Squinabol), and *Halesium* sp.

The *Turbocapsula costata* zone is defined by the EFAB of *Turbocapsula costata multicostata* Li and Matsuoka as the base and the last occurrence bio-horizon of *Turbocapsula costata* (Wu) as the top. The EFA of *T. costata costata* marks the evolution of *T. costata* and is used for subdividing the *Turbocapsula costata* zone into two subzones: the *Turbocapsula costata multicostata* subzone and the *Turbocapsula costata costata* subzone. The occurrence of *T. costata costata* in BB1-021 and GC-007 characterizes the *Turbocapsula costata costata* subzone.

A total of 21 species have been identified in red chert of BB1-021. The faunal contents are similar to those found in GC-007, which is red marl. Radiolarian assemblages, which are assignable to the *Turbocapsula costata costata* subzone, from the Umbria–Marche Basin and southern Tibet are characterized by the occurrences of *Thanarla brouweri* (Tan Sin Hok), *Stichomitra communis* Squinabol, *Turbocapsula costata costata* (Wu), *T. fugitiva*, *H. grutterinki*, *Squinabollum asseni* (Tan Sin Hok), *Pseudoeucyrtis hanni* (Tan Sin Hok), *Mictyoditra columbarium* (Renz), *Mesosaturnalis* sp., *Acastea* sp., *Suna* sp., *Archaeospongoprunum patricki* Jud, *Halesium* sp., *Conocaryomma* sp. B in Thurow (1988), and *Holocryptocanium tuberculatum* Dumitrica.

Within the *Aurisaturnalis carinatus perforatus* subzone in the Umbria–Marche Basin and southern Tibet, important and typical Early Cretaceous taxa occurring in older strata show their last occurrences: *A. lacrimula*, *A. excellens*, *Dictyomitra communis*, and *A. carinatus perforatus*. The last occurrences of these species are lower than the first occurrence of *T. costata costata*.

Common species in the *Aurisaturnalis carinatus perforatus* subzone and *Turbocapsula costata costata* subzone in both the Umbria–Marche Basin and southern Tibet are *S. communis*, *H. grutterinki*, *S. asseni*, *P. hanni*, *M. columbarium*，*Acastea* sp., *Suna* sp., *A. patricki*, and *Halesium* sp. The last occurrence of a large-sized species, *O. orca*, is a useful criterion for comparison and age assignment in the western Tethys (Aguado et al., 2014) and abundant in GC-025. However, it does not occur in corresponding strata in southern Tibet.

Suna echiodes, *A. diaphorogona*, and *S. hybum*, which possess three blade-like primary spines, show similar evolutionary trends from the *Aurisaturnalis carinatus* zone (GC-025) to the *Turbocapsula costata* zone both in southern Tibet and central Italy. Specimens of similar morphology, which possess thicker primary spines (Figs. 5.18, 5.19, 7.17, 7.18), are common in the *Turbocapsula costata* zone.

Radiolarian faunas in these two remote regions show a high similarity. Our new data shed light on a putative marine connection between the western Tethys and the eastern Tethys Himalayan region.

5.3. Radiolarian biostratigraphy and the early Aptian Oceanic Anoxic Event 1a (OAE 1a)

The biostratigraphic events of typical taxa in the Umbria–Marche Basin of western Tethys are compared to those in southern Tibet of the eastern Tethys. The radiolarian zones proposed in the Umbria–Marche Basin have been correlated with the magnetostratigraphic (Lowrie et al., 1980; Speranza et al., 2005; Satolli et al., 2007, 2008), nannofossil (Bralower et al., 1989; Monechi, 1989; Coccioni et al., 1992, 2012; Erba, 1994), and planktic foraminiferal (Coccioni et al., 1992, 2006；Patruno et al., 2015) biostratigraphic schemes. However, the BB1 section in southern Tibet is dominated by siliceous sediments, which contain no fossils other than radiolarians.

The early Aptian is a period of considerable environmental and climate change, during which activated seafloor spreading led to a high sea level and intense volcanic outgassing (Erba, 1994; Leckie et al., 2002; Erba et al., 2015). Organic-rich sediments associated with the early Aptian Oceanic Anoxic Event 1a (OAE 1a) were described from various marine basins, like the Alpine–Mediterranean regions (Coccioni et al., 1992; Pancost et al., 2004; Baudin et al., 1998), the central and southern Atlantic (Bralower et al., 1994), and the middle and northwestern Pacific (Sliter, 1989). The OAE 1a horizon, identified as the Selli Level, is located between GC-025 and GC-007 in the Gorgo a Cerbara section (Fig. 3). Based on radiolarian biostratigraphic comparison, the OAE 1a horizon is located between BB1-011 and BB1-020 in the BB1 section (Fig. 8). Black mudstone with high organic matter content is absent in a chert sequence in the Shimanto Belt in Japan (Ihoriya et al., 2009) and siliceous sequence in southern Tibet within the same biostratigraphically defined level. Accumulation of organic matter was clearly influenced by a variety of environmental factors peculiar to the basin.

O'Dogherty (1994) remarked that the FOB of *T. costata* (GC-911.35) is 13 m above the OAE 1a horizon. This study revises the FOB of *T. costata costata* as 6 m above the OAE 1a horizon. O'Dogherty (1994) remarked that the FOB of the genus *Turbocapsula* is within the OAE 1a horizon. Aguado et al. (2014) remarked that the FOB of the genus *Turbocapsula* is found in the lower Aptian just above the boundary between the Barremian and Aptian in XF1 section, southern Spain (Table 1). They also noted that the FOB of the genus *Turbocapsula* (= FOB of *T. fugitiva* or *T. tetras*) preceded the early Aptian OAE 1a. The OAE 1a horizon is located between the first appearance bio-horizon of the genus *Turbocapsula* and the EFAB of *T. costata costata*. OAE 1a should be located between BB1-011 and BB1-20 in BB1 section in southern Tibet (Fig. 8). Radiolarian faunal changes mentioned in chapter 5.1 coincide with the OAE 1a. Important and typical Early Cretaceous taxa, like *A. lacrimula, A. excellens, Dictyomitra communis,* and *A. carinatus perforatus* occurring in older strata show their last occurrence after the OAE 1a.

The onset of the OAE 1a is marked by a pronounced negative excursion in the $\delta^{13}C$ record, which is followed by a large, positive excursion (Weissert, 1989; Menegatti et al., 1998). This $\delta^{13}C$ record is a worldwide signal reflected by the global carbon cycle (Jenkyns, 1995; Adabi, 1997; Jarvis et al., 2006; Wendler, 2013). Low carbonate content makes the carbon-isotope analyses difficult for siliceous sequence in the southern Tibet. In the future, organic isotope chemostratigraphy is necessary for OAE 1a research on the siliceous sequence in southern Tibet.

6. Conclusion

Radiolarian assemblages from the two corresponding horizons of the Gorgo a Cerbara section and the Babazhadong 1 section are examined for comparison. Marls in the Gorgo a Cerbara section in the Umbria–Marche Basin in central Italy and a siliceous sequence (BB1 section) near Babazhadong in southern Tibet yield similar radiolarian faunas comparable to the *Aurisaturnalis carinatus* zone and *Turbocapsula* *costata* zone. Common species of these two zones in both sections are: *Dictyomitra communis* (Squinabol), *Hiscocapsa grutterinki* (Tan Sin Hok), *Squinabollum asseni* (Tan Sin Hok), *Pseudoeucyrtis hanni* (Tan Sin Hok), *Mictyoditra columbarium* (Renz), *Acastea* sp., *Suna* sp., *Archaeospongoprunum patricki* Jud, and *Halesium* sp. The zonation established based on the phyletic evolution of the genus *Turbocapsula* is applicable for the western Tethys. The OAE 1a horizon is located between the first appearance bio-horizon of the genus *Turbocapsula* and the EFAB of *T. costata costata*. Important and typical Early Cretaceous taxa, *A. lacrimula*, *A. excellens*, *Dictyomitra communis*, and *A. carinatus perforatus*, occurring in older strata show their last occurrences above the OAE 1a horizon.

ACKNOWLEDGMENTS

We thank editor Eduardo Koutsoukos, Špela Goričan, and an anonymous reviewer for carefully and critically reviewing our paper. This research was financially supported by the Chinese Academy of Sciences (CAS) Pioneer Hundred Talents Program; National Natural Science Foundation of China (grant number 41802013, 41572188 and 41772020); the Project of China Geological Survey (grant number 1212011086037 and 1212011121229); the National Natural Science Foundation of China (grant number 41572188 and 41772020); "Strategic Priority Research Program (B)" of the Chinese Academy of Sciences (Grant number XDB26000000); and the Japan Society for the Promotion of Science KAKENHI (grant numbers 15K05329 and 15H02142). We sincerely thank Wenjun Bi, Xiaohan

Li, and Xiaolong Zhang (China University of Geosciences, Beijing) for their cooperation in field work. We sincerely thank academic staff in Niigata University, especially the Earth History Seminar members for their support for our research.

References

Adabi, M.H., 1997. Application of carbon isotope chemostratigraphy to the Renison dolomites, Tasmania: a Neoproterozoic age. Australian Journal of Earth Sciences 44, 767–775.

Aguado, R., de Gea, G.A., O'Dogherty, L., 2014. Integrated biostratigraphy (calcareous nannofossils, planktonic foraminifera, and radiolarians) of an uppermost Barremian–lower Aptian pelagic succession in the Subbetic basin (southern Spain). Cretaceous Research 51, 153–173.

Baudin, F., Fiet, N., Coccioni, R., Galeotti, S., 1998. Organic matter characterisation of the Selli Level (Umbria–Marche Basin, central Italy). Cretaceous Research 19, 701–714.

Bralower, T.J, Monechi, S., Thierstein, H.R., 1989. Calcareous nannofossil zonation of the Jurassic–Cretaceous boundary interval and correlation with the geomagnetic polarity timescale. Marine Micropaleontology 14, 153–235.

Bralower, T.J., Arthur, M.A., Leckie, R.M., Sliter, W.V., Allard, D., Schlanger, S.O., 1994. Timing and paleocea nography of oceanic dysoxia/anoxia in the late Barremian to early Aptian, Palaios 9, 335–369.

Cecca, F., Pallini, G., Erba, E., Premoli-Silva, I., Coccioni, R., 1994. Hauterivian–

Barremian chronostratigraphy based on ammonites, nannofossils, planktic foraminifera and magnetic chrons from the Mediterranean domain. Cretaceous Research 15, 457–467.

Channell, J.E.T., D'Argenio, B., Horvath, F., 1979. Adria, the African promontory in Mesozoic Mediterranean palaeogeography. Earth-Science Reviews 15, 213–292.

Channell, J.E.T., Cecca, F., Erba, E., 1995. Correlation of Hauterivian and Barremian (Early Cretaceous) stage boundaries to polarity chrons. Earth Planet Science Letter 134, 125–140.

Coccioni, R., Erba, E., Premoli-Silva, I., 1992. Barremian–Aptian calcareous plankton biostratigraphy from the Gorgo a Cerbara section (Marche, central Italy) and implication for plankton evolution. Cretaceous Research 13, 457–467.

Coccioni, R., Luciani, V., Marsili, A., 2006. Cretaceous anoxic events and radially elongated chambered foraminifera: palaeoecological and palaeoceanographic implications. Palaeogeography, Palaeoclimatology, Palaeoecology 235, 66–92.

Coccioni, R., Jovane, L., Bancalà, G., Bucci, C., Fauth, G., Frontalini, F., Janikian, L., Savian, L., de Almeida, R.P., Mathias, G.L.M., da Trindade, R.I.F., 2012. Umbria–Marche Basin, central Italy: a reference section for the Aptian–Albian interval at low latitudes. Progress Reports of the Deep Sea Drilling Project 13, 42–46.

Du, X.J., Chen, X., Wang, C.S., Wei, Y.S., Li, Y.L., Jansa, L., 2015. Geochemistry and detrital zircon U-Pb dating of Lower Cretaceous volcaniclastics in the Babazhadong section, Northern Tethyan Himalaya: Implications for the breakup of Eastern Gondwana. Cretaceous Research 52, 127–137.

Dumitrica, P., Immenhauser, A., Dumitrica-Jud, R., 1997. Mesozoic radiolarian biostratigraphy from Masirah ophiolite, Sultanate of Oman. Bulletin of the national Museum of natural Science, Taiwan 9, 1–106.

Erba, E., 1994. Nannofossils and superplumes: the Early Aptian “nannoconid crisis”. Paleoceanography 9 (3), 483–501.

Erba, E., Duncan, R.A., Bottini, C., Tiraboschi, D., Weissert, H., Jenkyns, H.C., Malinverno, A., 2015. Environmental consequences of Ontong Java Plateau and Kerguelen Plateau volcanism. The Geological Society of America, special paper 511, pp. 271–303.

Erbacher, J., 1994. Entwicklung und Palaozeanographicmittelkretazischer Radiolarien der westlichen Tethys (Italien) und des Nordatlantiks. Tübinger Mikro-paläontologische Mitteilungen 12, pp. 1–88.

Gansser, A., 1964. Geology of the Himalayas. Wiley Interscience, London, pp. 1–289.

Hu, X.M., Jansa, L., Wang, C.S., 2008. Upper Jurassic–Lower Cretaceous stratigraphy in south-eastern Tibet: a comparison with the western Himalayas. Cretaceous Research 29, 301–315.

Ihoriya, N., Hori, R.E., Ikehara, M., 2009. Constraints upon anoxic water mass and variations in carbon isotopes during OAE1a (Early Cretaceous) from deep-sea sedimentary rocks of the Pacific Ocean News Osaka Micropaleontologists (NOM) 14, 297-315.

Jarvis, I., Gale, A.S., Jenkyns, H.C., Pearce, M.A., 2006. Secular variation in Late Cretaceous carbon isotopes: a new $\delta^{13}C$ carbonate reference curve for the

Cenomanian-Campanian (99.6–70.6 Ma). Geological Magazine 143, 561–608.

Jenkyns, H.C., 1995. Carbon-isotope stratigraphy and paleoceanographic significance of the Lower Cretaceous shallow-water carbonates of Resolution Guyot, Mid-Pacific Mountains. In: Winterer, E.L., Sager, W.W., Firth, J.V., Sinton, J.M. (Eds.), Proceedings of the Ocean Drilling Program. Scientific Results. vol. 143. Ocean Drilling Program, College Station, TX, pp. 99–104.

Leckie, R.M., Bralower, T.J., Cashman, R., 2002. Oceanic anoxic events and plankton evolution: biotic response to tectonic forcing during the mid-Cretaceous. Paleoceanography 17, 1041.

Li, X., Matsuoka, A., Li, Y., Wang, C., 2017. Phyletic evolution of the mid-Cretaceous radiolarian genus *Turbocapsula* from southern Tibet and its applications in zonation. Marine Micropaleontology 130, 29–42.

Liu, G., Einsele, G., 1994. Sedimentary history of the Tethyan basin in the Tibetan Himalayas. Geologische Rundschau 83, 32–61.

Lowrie, W., Alvarez, W., Premoli Silva, I., Monechi, S., 1980. Lower Cretaceous magnetic stratigraphy in Umbrian pelagic carbonate rocks. Geophysical Journal of the Royal Astronomical Society 60, 263–281.

Matsuoka, A., 1995. Jurassic and Lower Cretaceous radiolarian zonation in Japan and in the western Pacific. Island Arc 4 (2), 140–153.

Matsuoka, A., Yang, Q., Kobayashi, K., Takei, M., Nagahashi, T., Zeng, Q., Wang, Y., 2002. Jurassic–Cretaceous radiolarian biostratigraphy and sedimentary environments of the Ceno-Tethys: records from the Xialu Chert in the

Yarlung-Zangbo Suture Zone, southern Tibet. Journal of Asian Earth Sciences 20 (3), 277–287.

Monechi, S., 1989. Calcareous nannofossils and calpionellids of the Maiolica in the Bosso River section. In: Cresta, S., Monechi, S., Parisi, G. (Eds.), Mesozoic–Cenozoic Stratigraphy in the Umbria–Marche Area. Geological Field Trips in the Umbria–Marche Apennines (Italy). Memorie Descrittive della Carta Geologica d'Italia vol. XXXIX. Istituto Poligrafico e Zecca dello Stato, pp. 96–102.

Menegatti, A.P., Weissert, H., Brown, R.S., Tyson, R.V., Farrimond, P., Strasser, A., Caron,M., 1998. High resolution $\delta^{13}C$ stratigraphy through the early Aptian "Livello Selli" of the Alpine Tethys. Paleoceanography 13, 530–545.

Muttoni, G., Garzanti, E., Alfonsi, L., Cirilli, S., Germani, D., Lowrie, W., 2001. Motion of Africa and Adria since the Permian: paleomagnetic and paleoclimatic constraints from northern Libya. Earth and Planetary Science Letters 192, 159–174.

O'Dogherty, L., 1994. Biochronology and Paleontology of Mid-Cretaceous Radiolarians from Northern Apennines (Italy) and Betic Cordillera (Spain). Mémoires de Géologie (Lausanne) 21, 1–415.

Pancost, R.D., Crawford, N., Magness, S., Turner, A., Jenkyns, H.C., Maxwell, J.R., 2004. Further evidence for the development of photic-zone euxinic conditions during Mesozoic oceanic anoxic events, Journal of the Geological Society 161, 353–364.

Patruno, S., Kaminski, M.A., Coccioni, R., 2011. Agglutinated foraminifera from the proposed GSSP stratotype for the Barremian/Aptian boundary (Gorgo a Cerbara, Umbria–Marche basin, Italy. In: Filipescu, S., Kaminski, M.A. (Eds.), Proceedings of the Eighth International Workshop on Agglutinated Foraminifera. Grzybowski Foundation Special Publication 16, pp. 191–214.

Patruno, S, Triantaphyllou, M.V, Erba, E, Dimiza, M.D, Bottini, C, Kaminski, M.A., 2015. The Barremian and Aptian stepwise development of the 'Oceanic Anoxic Event 1a' (OAE 1a) crisis: integrated benthic and planktic high-resolution palaeoecology along the Gorgo a Cerbara stratotype section (Umbria–Marche Basin, Italy). Palaeogeography, Palaeoclimatology, Palaeoecology 424, 147–182.

Pessagno Jr, E.A., Newport, R.L., 1972. A technique for extracting Radiolaria from radiolarian cherts. Micropaleontology 18(2), 231–234.

Satolli, S., Besse, J., Speranza, F., Calamita, F., 2007. The 125–150 Ma high-resolution Apparent Polar Wander Path for Adria from magnetostratigraphic sections in Umbria Marche (Northern Apennines, Italy): timing and duration of the global Jurassic–Cretaceous hairpin turn. Earth Planet Science Letter 257, 329–342.

Satolli, S., Besse, J., Calamita, F., 2008. Paleomagnetism of Aptian–Albian sections from the Northern Apennines (Italy): implications for the 150–100 Ma apparent polar wander of Adria and Africa. Earth Planet Science Letter 276, 115–128.

Sliter, W.V., 1989. Aptian anoxia in the Pacific Basin, Geology 17, 909–912.

Speranza, F., Satolli, S., Mattioli, E., Calamita, F., 2005. Magnetic stratigraphy of Kimmeridgian–Aptian sections from Umbria–Marche (Italy): new details on the M polarity sequence. Journal of Geophysical Research B: Solid Earth 110 (12), 1–26.

Stein, M., Föllmi, K.B., Westermann, S., Godet, A., Adatte, T., Matera, V., Fleitmann, D., Berner, Z., 2011. Progressive palaeoenvironmental change during the Late Barremiane–EarlyAptian as prelude to Oceanic Anoxic Event 1a: evidence from the Gorgo a Cerbara section (Umbria–Marche basin, central Italy). Palaeogeography, Palaeoclimatology, Palaeoecology 302, 396–406.

Taketani, Y., 1982. Cretaceous radiolarian biostratigraphy of the Urakawa and Obira areas, Hokkaido Science Reports of the Tohoku University, Series 2, Geology 52 (1–2), 1–75.

Thurow, J., 1988. Cretaceous radiolarians of the North Atlantic Ocean: ODP Leg 103 (Sites 638, 640 and 641) and DSDP Legs 93 (Site 603) and 47B (Site 398). In: Boillot, G., Winterer, E. L. (Eds), Proceedings of the Ocean Drilling Program, Scientific Results, vol. 103, College Station, TX (Ocean Drilling Program), p. 379-418.

Wang, C.S., Xia, D.X., Zou, X., Chen, J.P., 1996. Field Trip Guide T121/T387, Geology Between the Indus-Yarlung Zangbo Suture Zone and the Himalaya Mountains (Xizang), China. Geological Publishing House, Beijing, pp. 1–72 (in Chinese, English abstract).

Wan, X., Zhao, W., Li, G., 2000. Restudy of the Upper Cretaceous in Gamba, Tibet. Geoscience 14, 281–285.

Weissert, H., 1989. C-isotope stratigraphy, a monitor of paleoenvironmental change: a case study from the Early Cretaceous. Surveys in Geophysics 10, 1–61.

Wendler, I., 2013. A critical evaluation of carbon isotope stratigraphy and biostratigraphic implications for Late Cretaceous global correlation. Earth-Science

Reviews 126, 116–146.

Wu, H.R., 1986. Some new genera and species of Cenomanian Radiolaria from southern Xizang (Tibet). Acta Micropalaeontologica Sinica 3, 347–359 (in Chinese with English abstract).

Wu, H.R., 2007. The Cretaceous radiolarian Turbocapsula costata zone and age of the chert sequences in Yarlung Zangbo suture zone, southern Tibet. Acta Micropalaeontologica Sinica 24 (4), 370–373 (in Chinese with English abstract).

Ziabrev, S., Aitchison, J., Abrajevitch, A., Davis, A., Luo, H., 2003. Precise radiolarian age constraints on the timing of ophiolite generation and sedimentation in the Dazhuqu terrane, Yarlung–Tsangpo suture zone, Tibet. Journal of the Geological Society 160 (4), 591–599.

Ziabrev, S.V., Aitchison, J.C., Abrajevitch, A.V., Davis, A.M., Luo, H., 2004. Bainang terrane, Yarlung–Tsangpo suture, southern Tibet (Xizang, China): a record of intra-Neotethyan subduction–accretion processes preserved on the roof of the world. Journal of the Geological Society 161 (3), 523–539.

Caption

Figure 1. Locations of the Babazhadong 1 section in southern Tibet (location 1) and the Gorgo a Cerbara section in central Italy (location 2).

Figure 2. Early Aptian palaeogeographic reconstruction (ODSN Plate Tectonic Reconstruction Service http://www.odsn.de/odsn/services/paleomap/paleomap.html) showing the locations of the Babazhadong 1 section in southern Tibet (location 1) and the Gorgo a Cerbara section in central Italy (location 2).

Figure 3. Lithologic columns of the Gorgo a Cerbara section according to Patruno et al. (2011; 2015). Biostratigraphic occurrence of typical species of O'Dogherty (1994) and this study for the Gorgo a Cerbara section. Dots = this study; lines = occurrence according to O'Dogherty (1994).

Figure 4. Scanning electron micrographs of biostratigraphically relevant radiolarians from sample BB1-011 (*Aurisaturnalis carinatus perforatus* subzone) in the Babazhadong 1 section. For each illustration the caption includes the photo number and the stub position in brackets. 1. *Archaeodictyomitra lacrimula* (Foreman), 036536-1155-3-19. 2. *Archaeodictyomitra excellens* (Tan Sin Hok), 036521-1155-1-1. 3. *Dictyomitra communis* (Squinabol), 044112-1046-12-25. 4. *Pseudocrolanium puga* (Schaaf), 044099-1046-7-24. 5. *Acaeniotyle umbilicata* (Rüst), 036553-1155-7-12. 6. *Aurisaturnalis carinatus perforatus* Dumitrica and Dumitrica–Jud, 1995, 036548-1155-5-16. 7. *Dicerosaturnalis amissus* (Squinabol), 039559-1214-2-7. 8. *Pseudodictyomitra recta* Vishnevskaya, 044095-1046-6-1. 9. *Stichomitra communis* Squinabol, 044082-1046-2-9. 10. *Neorelumbra manokawaensis* (Tumanda), 044105-1046-9-24. 11. *Thanarla pacifica* Nakaseko and Nishimura, 044091-1046-4-16. 12. *Xitus alievi* (Foreman), 039582-1214-7-3. 13. *Squinabollum asseni* (Tan Sin Hok), 044128-1050-6-3. 14. *Hiscocapsa grutterinki* (Tan Sin Hok), 036539-1155-4-8. 15. *Arcanicapsa clivosa* (Aliev), 039552-1214-1-4. 16. *Turbocapsula tetras* Li and Matsuoka. 17. *Pseudoeucyrtis hanni* (Tan Sin Hok), 044100-1046-7-25. 18. *Mictyoditra columbarium* (Renz), 036557-1155-8-6. 19. *Suna echiodes* (Foreman), 039590-1214-8-5. 20. *Acastea diaphorogona* (Foreman),

044115-1046-14-1. 21. *Quinquecapsularia* sp., 044090-1046-4-11. 22. *Conocaryomma* sp. B in Thurow, 044086-1046-3-17. 23. *Dactyliosphaera* sp., 036551-1155-6-8. 24. *Becus horridus* (Squinabol), 044089-1046-4-10. 25. *Emiluvia* sp., 044118-1046-4-9. 26. *Halesium* sp., 044123-1050-3-4. 27. *Archaeospongoprunum patricki* Jud, 039560-1214-3-2.

Figure 5. Scanning electron micrographs of biostratigraphically relevant radiolarians from sample BB1-021 (*Turbocapsula costata costata* Subzone) in the Babazhadong 1 section. For each illustration the caption includes the photo number and the stub position in brackets. 1. *Thanarla brouweri* (Tan Sin Hok), 044251-1321-1-3. 2. *Pseudocrolanium puga* (Schaaf), 044256-1321-2-7. 3. *Pseudodictyomitra recta* Vishnevskaya, 044253-1321-1-6. 4. *Pseudodictyomitra hornatissima* (Squinabol), 044254-1321-2-1. 5. *Xitus clava* (Parona), 044258-1321-2-9. 6. *Stichomitra communis* Squinabol, 044260-1321-3-2. 7. *Turbocapsula costata costata* (Wu), 042479-1215-9-15. 8. 9. *Turbocapsula fugitiva* O'Dogherty, 8. 044266-1321-4-5, 9. 044271-1321-5-3. 10. *Hiscocapsa grutterinki* (Tan Sin Hok), 044272-1321-5-4. 11. *Squinabollum asseni* (Tan Sin Hok), 044268-1321-4-9. 12. *Pseudoeucyrtis hanni* (Tan Sin Hok), 044276-1321-6-2. 13. *Mictyoditra columbarium* (Renz), 044277-1321-6-5. 14. *Mesosaturnalis* sp., 036737-1158-10-6. 15. *Dicerosaturnalis amissus* (Squinabol), 036739-1158-10-8. 16. *Acastea diaphorogona* (Foreman), 039436-1215-1-7. 17. *Suna hybum* (Foreman), 039439-1215-2-2. 18. *Acastea* sp., 044281-1321-6-12. 19. *Suna* sp., 044284-1321-7-4. 20. *Becus horridus* (Squinabol), 039486-1215-7-13. 21. *Pantanellium squinaboli* (Tan Sin Hok), 039500-1215-10-13. 22. *Archaeospongoprunum patricki* Jud, 044286-1321-7-9. 23. *Acaeniotyle umbilicata* (Rüst), 044259-1321-2-13. 24. *Halesium* sp., 044285-1321-7-5. 25. *Conocaryomma* sp. B in Thurow, 039431-1215-1-1. 26. *Holocryptocanium tuberculatum* Dumitrica, 039523-1215-13-12. 27. *Conocaryomma* sp., 044295-1321-8-13. 28. *Deviatus diamphidius* (Foreman), 044288-1321-8-1.

Figure 6. Scanning electron micrographs of biostratigraphically relevant radiolarians from sample GC-025 (*Aurisaturnalis carinatus perforatus* Subzone) in the Gorgo a Cerbara section. For each illustration the caption includes the photo number and the

stub position in brackets. 1. *Archaeodictyomitra lacrimula* (Foreman), 043664-1289-9-1. 2. *Archaeodictyomitra excellens* (Tan Sin Hok), 043640-1289-7-6. 3. *Dictyomitra communis* (Squinabol), 043595-1289-3-7. 4. *Crococapsa uterculus* (Parona), 043649-1289-8-1. 5. *Olanda orca* (Foreman), 043482-1288-1-2. 6. *Pantanellium squinaboli* (Tan Sin Hok), 043612-1289-4-14. 7. *Acaeniotyle umbilicata* (Rüst), 043495-1288-3-5. 8. *Aurisaturnalis carinatus perforatus* Dumitrica and Dumitrica–Jud, 043523-1288-6-1. 9. *Dicerosaturnalis amissus* (Squinabol), 043529-1288-6-7. 10. *Thanarla pacifica* Nakaseko and Nishimura, 043676-1289-10-3. 11. *Pseudodictyomitra nodocostata* Dumitrica, 043596-1289-3-8. 12. *Pseudodictyomitra nakasekoi* Taketani, (This specimen looks like *Pseudodictyomitra nakasekoi* Taketani. However, the first appearance of this species is recorded as Cenomanian in Taketani (1982). This possibly because Cenomanian strata are the bottom of his sections.) 043556-1288-9-7. 13. *Xitus clava* (Parona), 043569-1288-10-9. 14. *Stichomitra communis* Squinabol, 043588-1289-2-13. 15. *Neorelumbra manokawaensis* (Tumanda), 043641-1289-7-7. 16. *Squinabollum asseni* (Tan Sin Hok), 043650-1289-8-3. 17. *Hiscocapsa grutterinki* (Tan Sin Hok), 043642-1289-7-8. 18. *Arcanicapsa clivosa* (Aliev), 043627-1289-6-6. 19. *Hiscocapsa*? sp., 044075-1308-3-2. 20. *Pseudoeucyrtis hanni* (Tan Sin Hok), 043582-1289-2-7. 21. *Mictyoditra columbarium* (Renz), 043658-1289-8-10. 22. *Acastea diaphorogona* (Foreman), 043498-1288-3-7. 23. *Suna hybum* (Foreman), 043603-1289-4-4. 24. *Quinquecapsularia* sp., 043501-1288-4-1. 25. *Dactyliodiscus* sp., 043544-1288-8-5. 26. *Becus horridus* (Squinabol), 043644-1289-7-11. 27. *Conocaryomma* sp. B in Thurow, 043548-1288-8-11. 28. *Staurosphaeretta* sp., 043611-1289-4-12. 29. *Halesium* sp., 043500-1288-3-9. 30. *Dicroa macroxiphus* (Rüst) 043655-1289-8-7.

Figure 7. Scanning electron micrographs of biostratigraphically relevant radiolarians from sample GC-007 (*Turbocapsula costata costata* Subzone) in the Gorgo a Cerbara section. For each illustration the caption includes the photo number and the stub position in brackets. 1, 2. *Thanarla brouweri* (Tan Sin Hok), 043753-1290-1-6. 2. 043757-1290-2-3. 3. *Dictyomitra communis* (Squinabol), 043755-1290-1-10. 4. *Pseudocrolanium puga* (Schaaf), 043796-1290-7-5. 5. *Pseudodictyomitra*

hornatissima (Squinabol), 043798-1290-7-13. 6. *Xitus clava* (Parona), 043752-1290-1-5. 7–9. *Turbocapsula costata costata* (Wu), 7. 043764-1290-3-4, 8. 043767-1290-3-8, 9. 043780-1290-5-4. 10. *Hiscocapsa*? sp., 043774-1290-4-5. 11. *Hiscocapsa grutterinki* (Tan Sin Hok), 043791-1290-6-11. 12. *Squinabollum asseni* (Tan Sin Hok), 043800-1290-8-3. 13. *Hiscocapsa* sp., 043786-1290-5-13. 14. *Pseudoeucyrtis hanni* (Tan Sin Hok). 15. *Mictyoditra columbarium* (Renz), 043820-1290-10-2. 16. *Mesosaturnalis* sp. 043810-1290-8-15. 17. *Acastea* sp., 043812-1290-9-3. 18. *Suna* sp., 043797-1290-7-12. 19. *Archaeospongoprunum patricki* Jud, 043821-1290-10-3. 20. *Halesium* sp., 043751-1290-1-2. 21. *Conocaryomma* sp. B in Thurow (1988), 043790-1290-6-9. 22. *Holocryptocanium tuberculatum* Dumitrica, 043794-1290-7-3. 23. *Dactyliodiscus florealis* (Jud), 043787-1290-6-1.

Figure 8. Comparison of the Gorgo a Cerbara section and BB1 section based on radiolarian biostratigraphy. For BB1 section, A. grayish-green cherts interbedded with claystones, B. red and green cherts interbedded with claystones, C. red cherts interbedded with claystones.

Table 1. Occurrence of radiolarian species in the Gorgo a Cerbara (GC) section of O’Dogherty (1994) and this study, the Babazhadong 1 (BB1) section of this study, and the XF1 section of Aguado et al. (2014).

Table 1 Occurrence of radiolarian species in the Gorgo a Cerbara (GC) section of O'Dogherty (1994) and this study, the Babazhadong (BB1) section of this study, and the XF1 section of Aguado et al. (2014).

References	O'Dogherty (1994)						This study				Aguado et al. (2014)		
Section	GC section						GC section		BB1 section		XF1 section		
Sample Number	893.30	896.70	899.75	902.40	911.35	914.00	025	007	011	021	0.70	12.00	30.10
Archaeodictyomitra lacrimula (Foreman)	○	○	○				○		○		○	○	
Archaeodictyomitra excellens (Tan Sin Hok)	○	○	○				○		○				
Dictyomitra communis (Squinabol)	○	○	○	○	○	○	○	○	○		○	○	
Thanarla pacifica Nakaseko and Nishimura	○	○	○	○			○		○				
Thanarla brouweri (Tan Sin Hok)		○			○	○		○		○			
Pseudodictyomitra nodocostata Dumitrica							○						○
Pseudodictyomitra recta Vishnevskaya									○	○			
Pseudodictyomitra hornatissima (Squinabol)	○	○	○		○	○		○		○			○
Pseudodictyomitra nakasekoi Taketani							○						
Pseudocrolanium puga (Schaaf)								○	○	○			
Stichomitra communis Squinabol			○				○		○	○			○
Neorelumbra manokawaensis (Tumanda)							○		○				
Xitus alievi (Foreman)	○	○							○				
Xitus clava (Parona)	○		○	○	○		○	○		○			
Turbocapsula tetras Li and Matsuoka									○				
Turbocapsula fugitiva O'Dogherty		○			○	○				○	?		○
Turbocapsula costata multicostata Li and Matsuoka													
Turbocapsula costata costata (Wu)					?	?		○		○			○
Squinabollum asseni (Tan Sin Hok)	○	○		○	○	○	○	○	○	○			
Hiscocapsa grutterinki (Tan Sin Hok)	○	○	○	○	○	○	○	○	○	○			
Crococapsa uterculus (Parona)	○		○				○						
Arcanicapsa clivosa (Aliev)	○	○	○	○	○		○		○		○	○	○
Olanda orca (Foreman)							○				○		
Pseudoeucyrtis hanni (Tan Sin Hok)	○	○	○	○	○	○		○	○	○			
Mictyoditra columbarium (Renz)	○	○	○	○	○	○		○	○	○			
Aurisaturnalis carinatus perforatus Dumitrica and Dumitrica–Jud	?	?					○		○				
Suna echiodes (Foreman)									○				
Suna hybum (Foreman)	○			○	○		○			○			
Acastea diaphorogona (Foreman)	○	○	○	○	○	○	○		○	○			
Acaeniotyle umbilicata (Rüst)	○	○	○	○	○	○	○		○	○	○	○	
Archaeospongoprunum patricki Jud	○	○						○	○	○			
Dicroa (?) *macroxiphus* (Rüst)							○						
Pantanellium lanceola (Parona)	○	○	○										
Pantanellium squinaboli (Tan Sin Hok)							○			○			
Dicerosaturnalis amissus (Squinabol)	○	○	○	○	○	○	○		○	○			
Becus horridus (Squinabol)					○		○		○	○			
Becus gemmatus Wu	○					○						○	
Crucella hispana O'Dogherty					○	○						○	
Holocryptocanium tuberculatum Dumitrica								○		○			
Deviatus diamphidius (Foreman)	○	○		○	○					○			
Dactyliodiscus florealis (Jud)								○			○		

○, species identified with certainty; ?, species identified with some doubt.

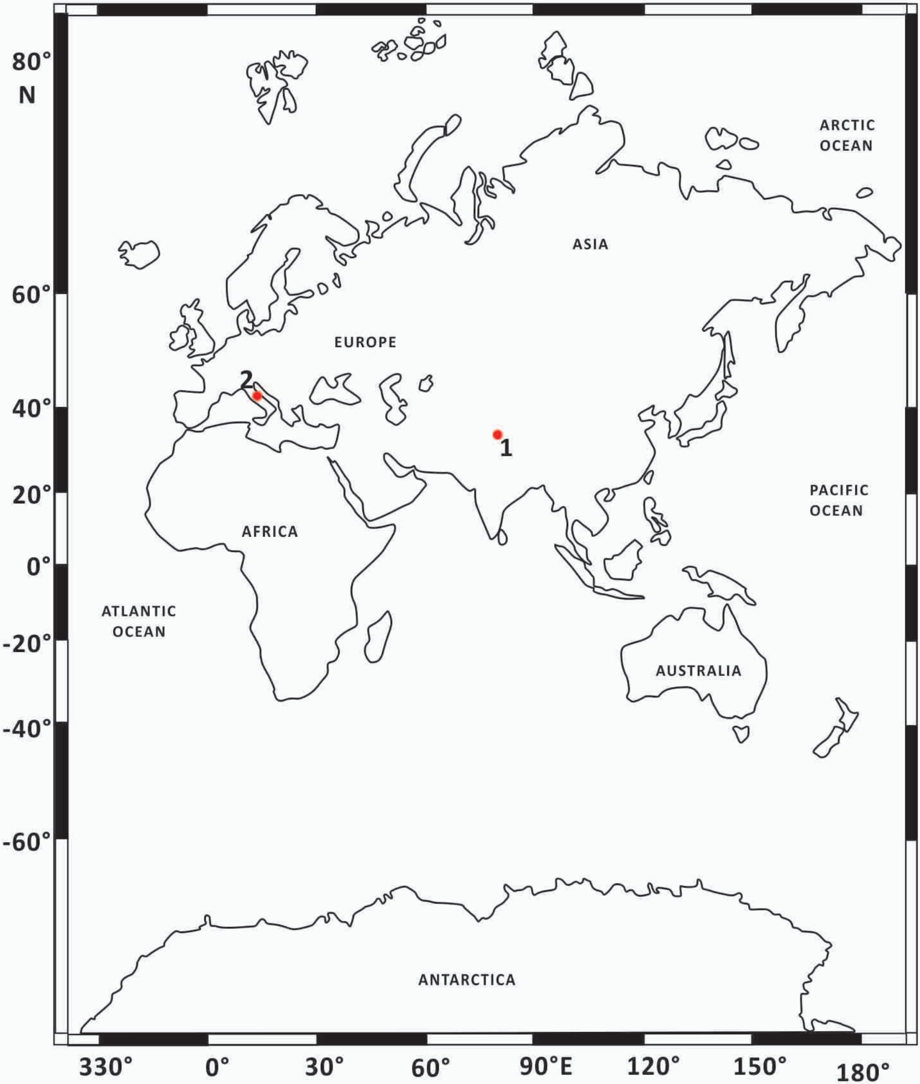
80° N
60°
40°
20°
0°
-20°
-40°
-60°
330°
0°
30°
60°
90°E
120°
150°
180°
ARCTIC OCEAN
ASIA
EUROPE
2
1
PACIFIC OCEAN
AFRICA
ATLANTIC OCEAN
AUSTRALIA
ANTARCTICA

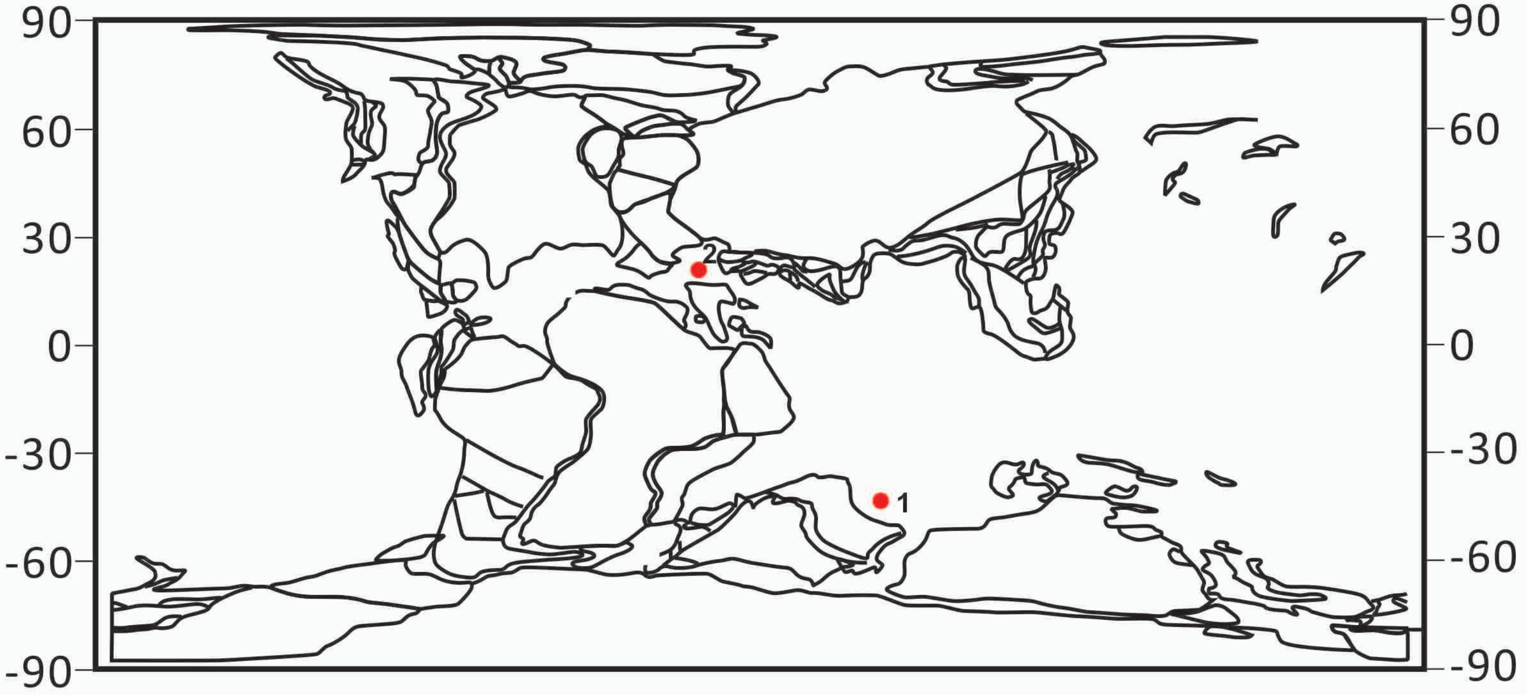
90
60
30
0
-30
-60
-90
90
60
30
0
-30
-60
-90
1
2

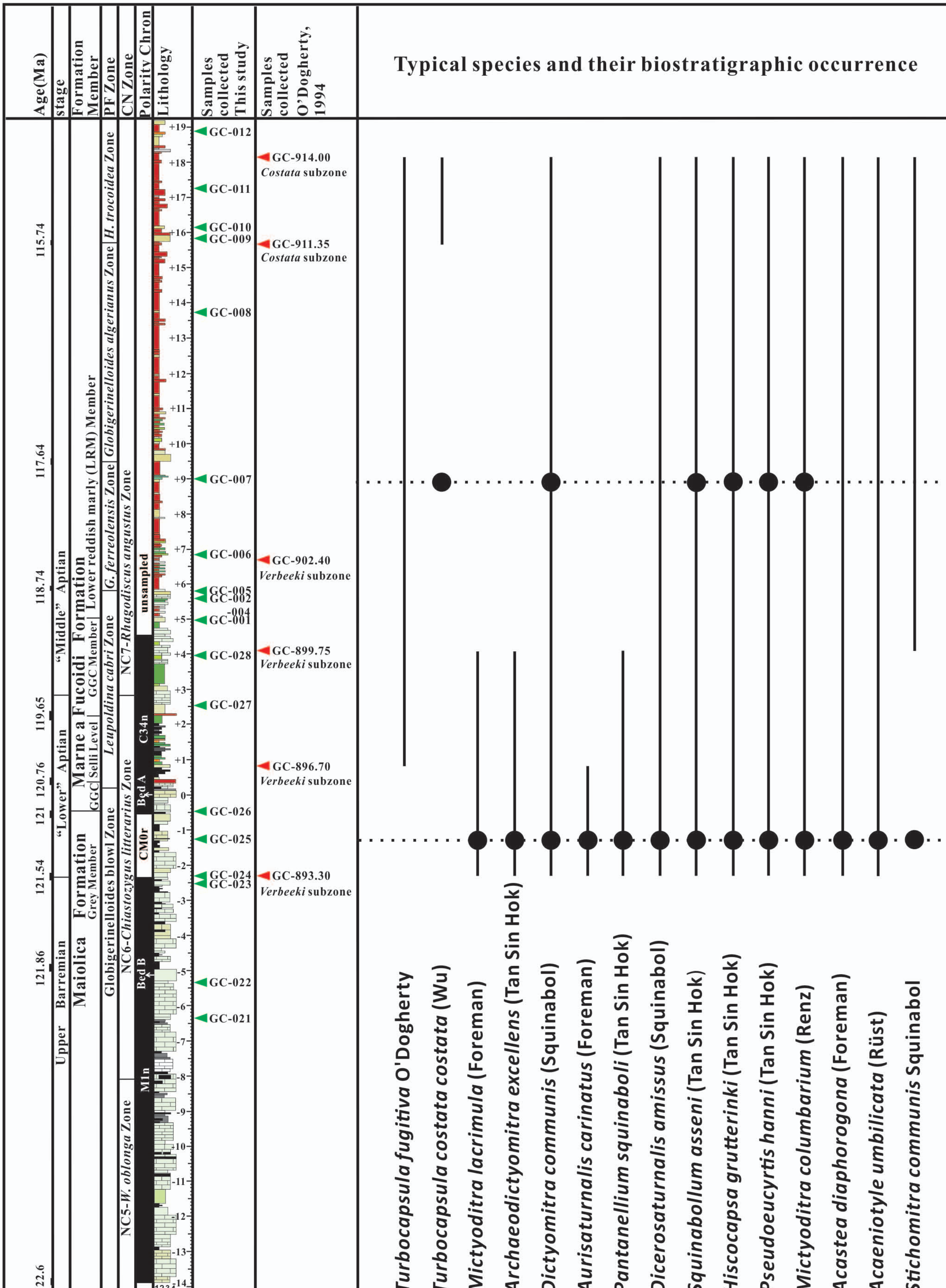

Age(Ma)
stage
Formation Member
PF Zone
CN Zone
Polarity Chron
Lithology
Samples collected This study
Samples collected O'Dogherty, 1994
Typical species and their biostratigraphic occurrence
115.74
117.64
118.74
119.65
120.76
121
121.54
121.86
122.6
Upper Barremian
"Lower" Aptian
"Middle" Aptian
Maiolica Formation
Grey Member
Marne a Fucoidi Formation
GGC Selli Level
GGC Member
Lower reddish marly (LRM) Member
Globigerinelloides blowi Zone
Leupoldina cabri Zone
G. ferreolensis Zone
Globigerinelloides algerianus Zone
H. trocoidea Zone
NC5-W. oblonga Zone
NC6-Chiastozygus litterarius Zone
NC7-Rhagodiscus angustus Zone
M1n
CM0r
C34n
Bed A
Bed B
unsampled
1234
GC-012
GC-011
GC-010
GC-009
GC-008
GC-007
GC-006
GC-005
GC-002
-004
GC-001
GC-028
GC-027
GC-026
GC-025
GC-024
GC-023
GC-022
GC-021
GC-914.00
Costata subzone
GC-911.35
Costata subzone
GC-902.40
Verbeeki subzone
GC-899.75
Verbeeki subzone
GC-896.70
Verbeeki subzone
GC-893.30
Verbeeki subzone
Turbocapsula fugitiva O'Dogherty
Turbocapsula costata costata (Wu)
Mictyoditra lacrimula (Foreman)
Archaeodictyomitra excellens (Tan Sin Hok)
Dictyomitra communis (Squinabol)
Aurisaturnalis carinatus (Foreman)
Pantanellium squinaboli (Tan Sin Hok)
Dicerosaturnalis amissus (Squinabol)
Squinabollum asseni (Tan Sin Hok)
Hiscocapsa grutterinki (Tan Sin Hok)
Pseudoeucyrtis hanni (Tan Sin Hok)
Mictyoditra columbarium (Renz)
Acastea diaphorogona (Foreman)
Acaeniotyle umbilicata (Rüst)
Stichomitra communis Squinabol

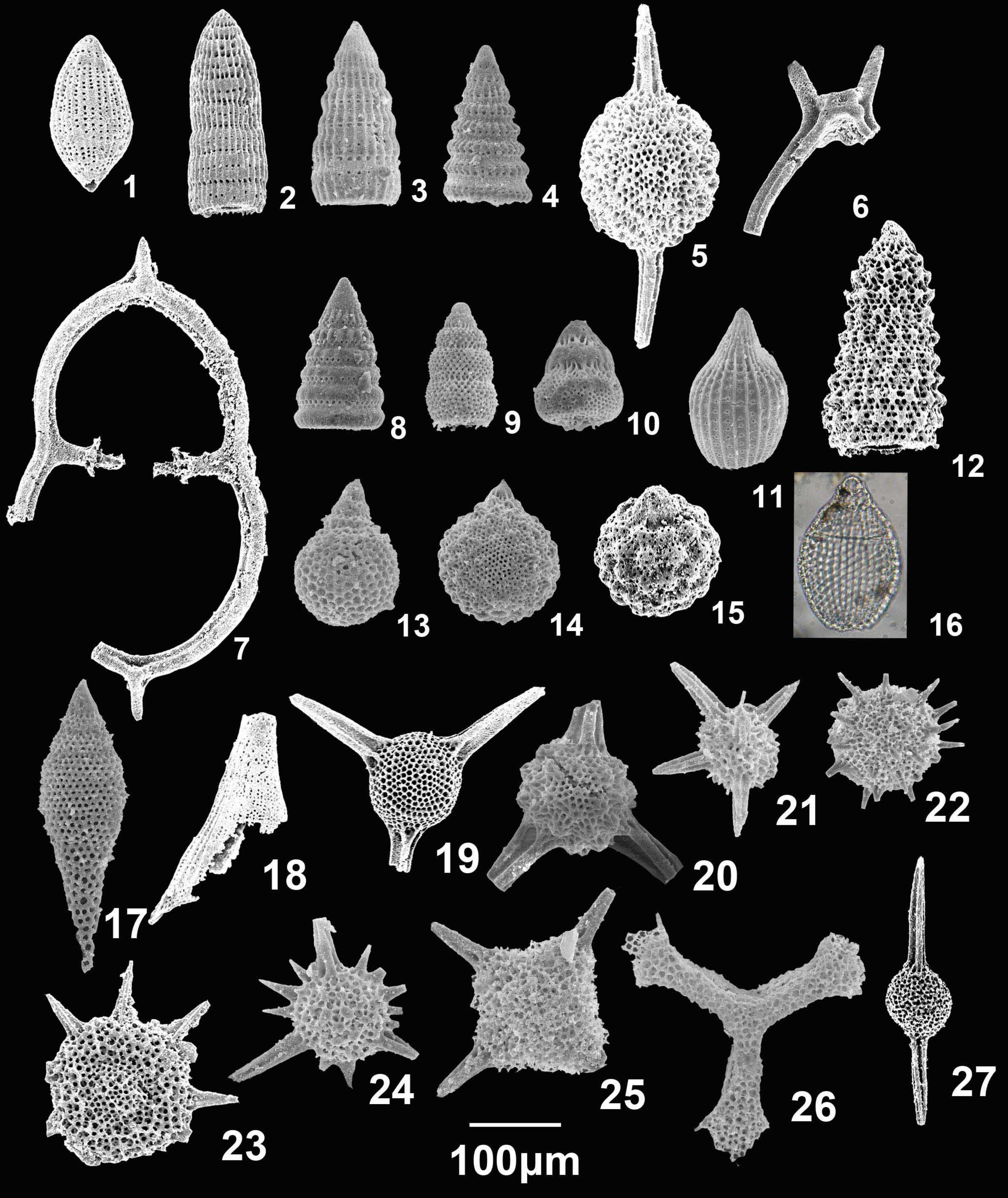
1
2
3
4
5
6
7
8
9
10
11
12
13
14
15
16
17
18
19
20
21
22
23
24
25
26
27
100µm

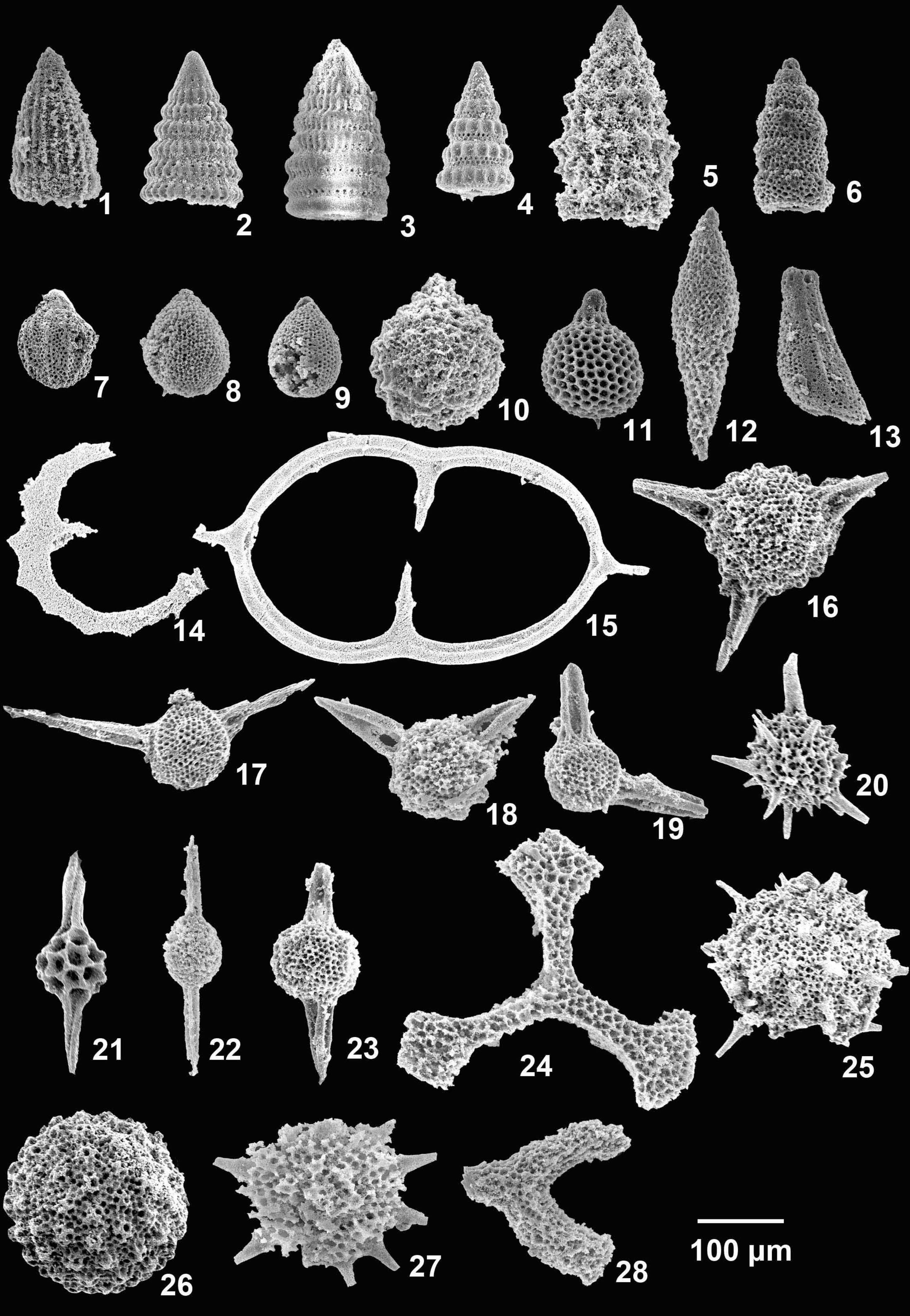
1
2
3
4
5
6
7
8
9
10
11
12
13
14
15
16
17
18
19
20
21
22
23
24
25
26
27
28
100 µm

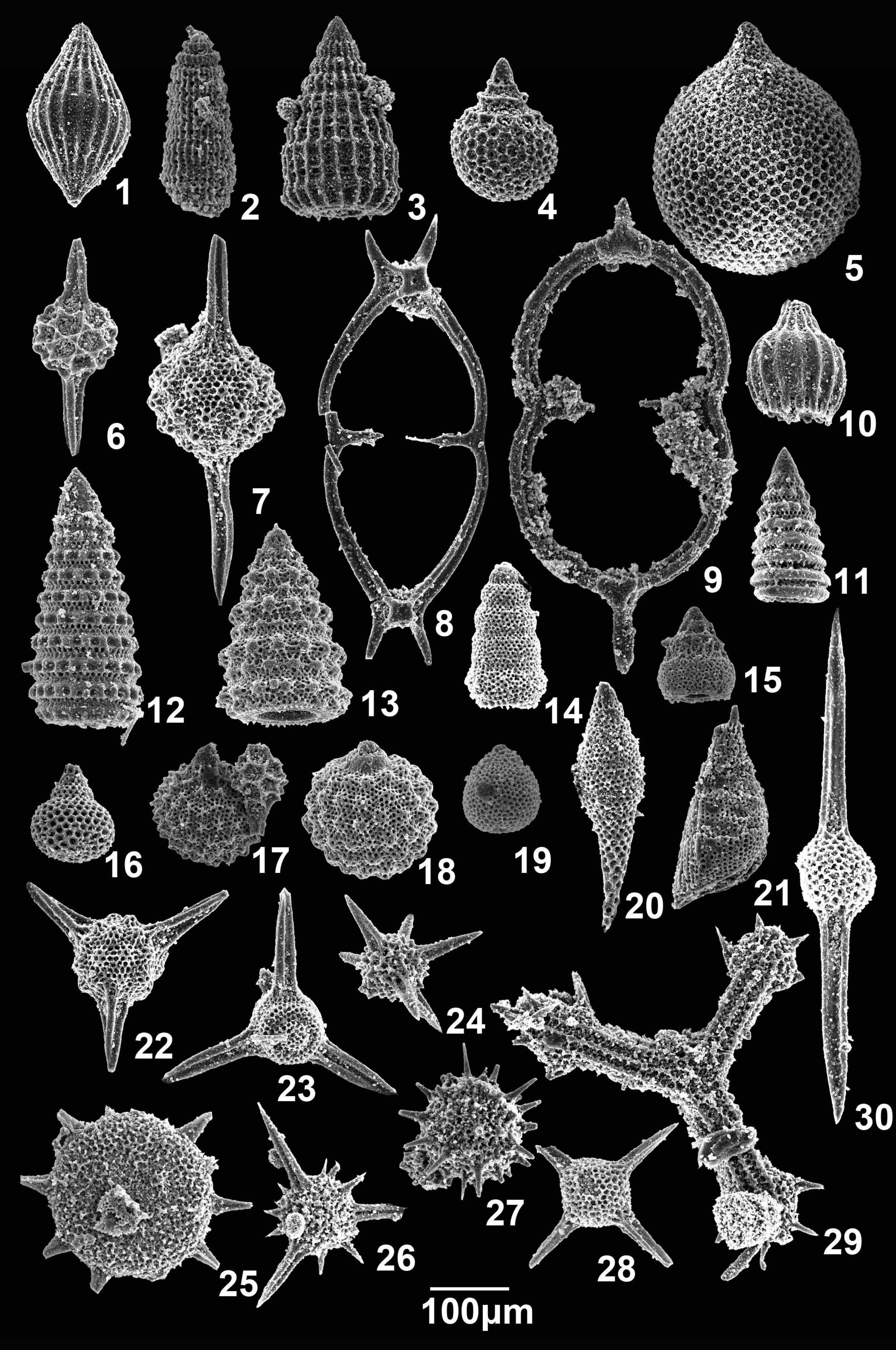
1
2
3
4
5
6
7
8
9
10
11
12
13
14
15
16
17
18
19
20
21
22
23
24
25
26
27
28
29
30
100µm

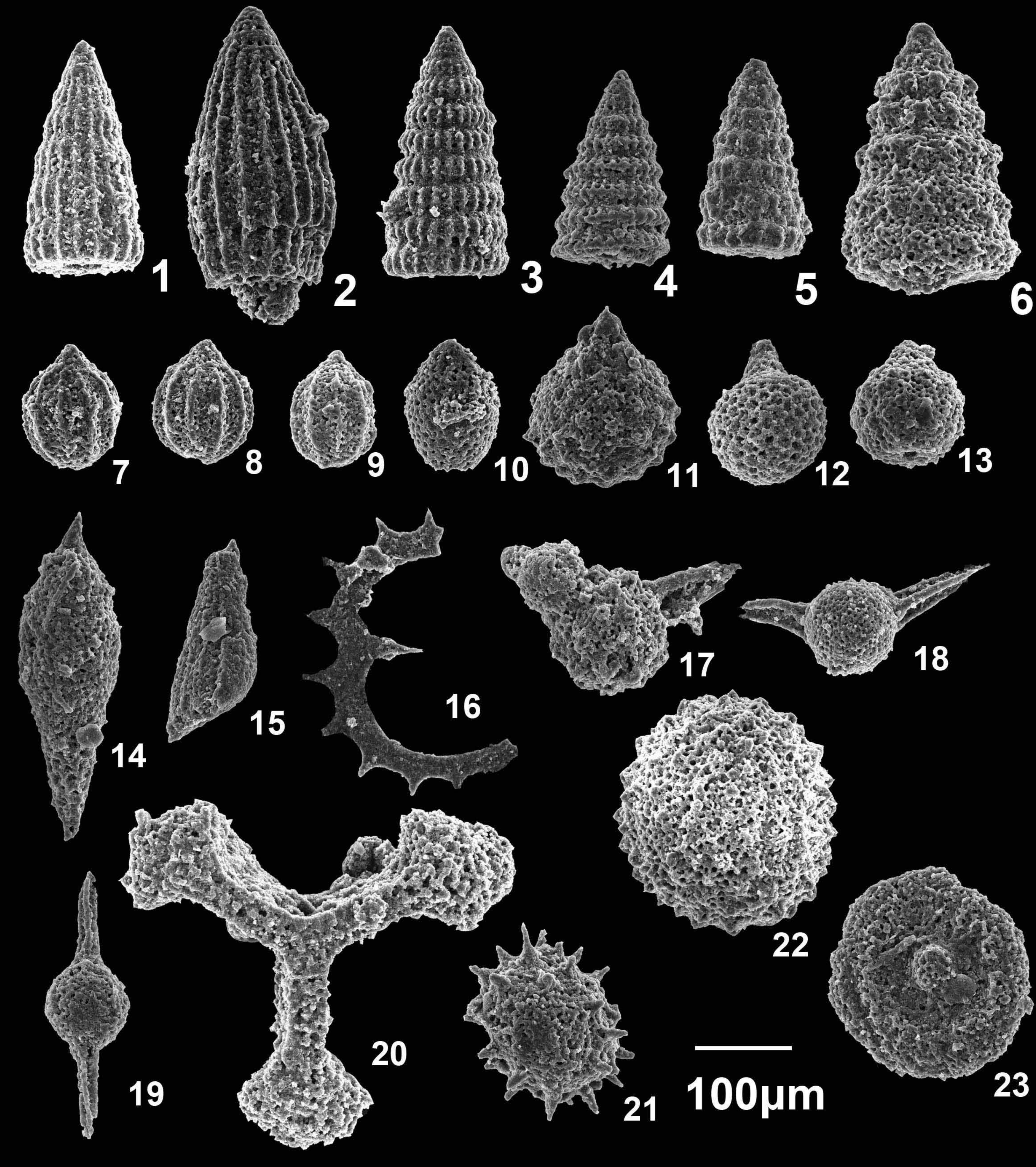
1
2
3
4
5
6
7
8
9
10
11
12
13
14
15
16
17
18
19
20
21
22
23
100µm

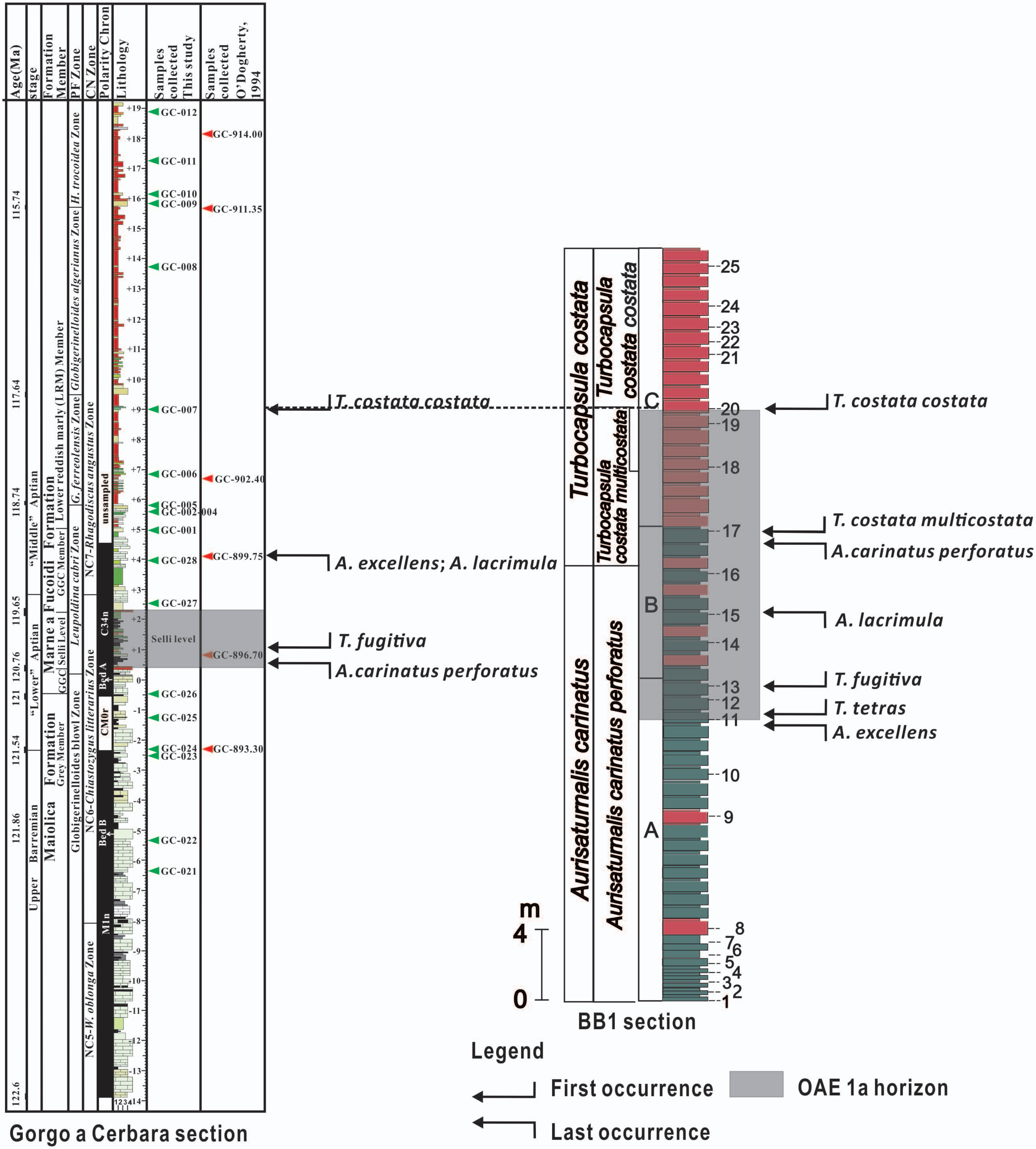

Age(Ma)
stage
Formation Member
PF Zone
CN Zone
Polarity Chron
Lithology
Samples collected This study
Samples collected O'Dogherty, 1994
115.74
117.64
118.74
119.65
120.76
121
121.54
121.86
122.6
"Middle" Aptian
"Lower" Aptian
Upper Barremian
Marne a Fucoidi Formation
Maiolica Formation
Lower reddish marly (LRM) Member
GGC Member
Selli Level
GGC
Grey Member
H. trocoidea Zone
Globigerinelloides algerianus Zone
G. ferreolensis Zone
Leupoldina cabri Zone
Globigerinelloides blowi Zone
NC7-Rhagodiscus angustus Zone
NC6-Chiastozygus litterarius Zone
NC5-W. oblonga Zone
unsampled
C34n
Bed A
CM0r
Bed B
M1n
Selli level
GC-012
GC-011
GC-010
GC-009
GC-008
GC-007
GC-006
GC-005
GC-002-004
GC-001
GC-028
GC-027
GC-026
GC-025
GC-024
GC-023
GC-022
GC-021
GC-914.00
GC-911.35
GC-902.40
GC-899.75
GC-896.70
GC-893.30
T. costata costata
A. excellens; A. lacrimula
T. fugitiva
A.carinatus perforatus
Gorgo a Cerbara section
Turbocapsula costata
Turbocapsula costata costata
Turbocapsula costata multicostata
Aurisaturnalis carinatus
Aurisaturnalis carinatus perforatus
C
B
A
m
4
0
BB1 section
T. costata costata
T. costata multicostata
A.carinatus perforatus
A. lacrimula
T. fugitiva
T. tetras
A. excellens
Legend
First occurrence
Last occurrence
OAE 1a horizon